

Damage distributions in GaAs single crystal irradiated with ^{84}Kr (394 MeV), ^{209}Bi (710 MeV) and ^{238}U (1300 MeV) swift ions

Alexander Yu. Didyk,
Fadei F. Komarov,
Ludmila A. Vlasukova,
Evgenia A. Gracheva,
Andrzej Hofman,
Vera N. Yuvchenko,
Roland Wiśniewski,
Teresa Wilczyńska

Abstract. We are presenting a study of damage distribution in GaAs irradiated with ^{84}Kr ions of energy $E_{\text{Kr}} = 394$ MeV up to the fluence of 5×10^{12} ion/cm². The distribution of damage along the projected range of ^{84}Kr ions in GaAs was investigated using selective chemical etching of a single crystal cleaved perpendicularly to the irradiated surface. The damage zone located under the Bragg peak of ^{84}Kr ions was observed. Explanation of the observed effects based on possible processes of channeling of knocked target atoms (Ga and As) is proposed.

Key words: semiconductors • gallium arsenide • swift heavy ions • inelastic energy loss • atomic force microscopy (AFM) • ion channeling

A. Yu. Didyk✉
Flerov Laboratory of Nuclear Reaction,
Joint Institute of Nuclear Research,
6 Joliot-Curie Str., 141980 Dubna, Russia,
Tel.: +7 49621 63376, Fax: +7 49621 65083,
E-mail: didyk@jinr.ru

F. F. Komarov, L. A. Vlasukova, E. A. Gracheva,
V. N. Yuvchenko
Belarusian State University,
4 Nezavisimosti Ave., 220030 Minsk, Belarus

A. Hofman
Joint Institute of Nuclear Research,
6 Joliot-Curie Str., 141980 Dubna, Russia
and Institute of Atomic Energy,
05-400 Otwock-Świerk, Poland

R. Wiśniewski, T. Wilczyńska
Institute of Atomic Energy,
05-400 Otwock-Świerk, Poland

Received: 28 September 2007
Accepted: 28 April 2008

Introduction

Unique properties of nanometer structures such as quantum dots, wires and so on have attracted a great interest for some decades [1, 14]. One way of nanometer structuring of solids is swift heavy ion irradiation. Under the definite conditions it creates an ion tracks system in the form of narrow cylinders or nanometer cluster chains with modified structure embedded into undamaged matrix. The study of interaction of swift heavy ions with semiconductor single crystals is very important both for the fundamental investigations of radiation effects in condensed matter and for the creation of ion tracks in semiconductor materials, which can be used in modern nanotechnologies of electronics [2, 5–7, 13, 15].

In this paper we present a study of radiation damage in GaAs single crystals irradiated with ^{84}Kr ions of energy $E_{\text{Kr}} = 394$ MeV up to the fluence of $(\Phi \times t)_{\text{Kr}} = 5 \times 10^{12}$ ion/cm² and possible explanation of observed effects.

Experimental methods and results

The samples of GaAs single crystals of square $S = 1$ cm² and a thicknesses of 300 and 400 μm were prepared by high quality mechanical and chemical polishing treatments and then irradiated with ^{84}Kr ions perpendicularly to the surface in the U-400 heavy ion accelerator of the Flerov Laboratory of Nuclear Reaction (Joint Institute of Nuclear Research, Dubna). The ion energy was $E_{\text{Kr}} =$

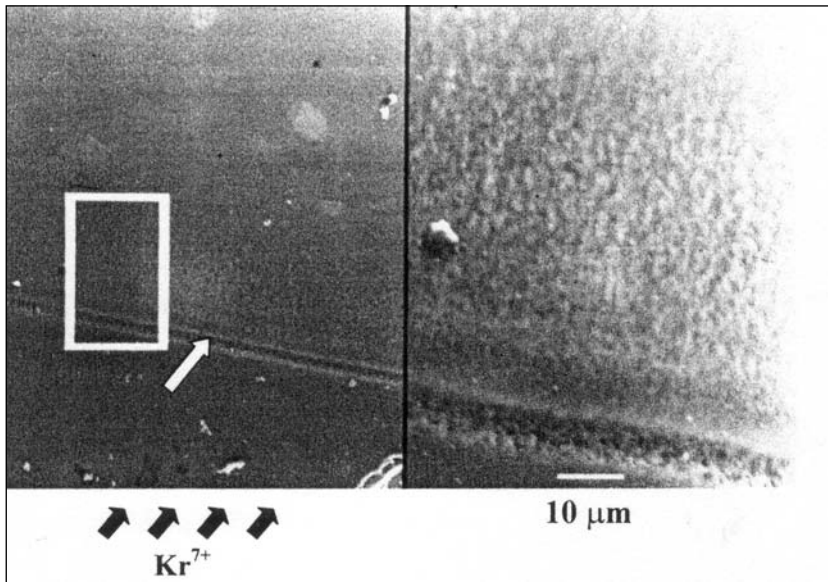


Fig. 1. SEM images of etched cross section cleave of GaAs sample irradiated with ^{84}Kr ions ($E_{\text{Kr}} = 394 \text{ MeV}$, $(\Phi \times t)_{\text{Kr}} = 5 \times 10^{12} \text{ ion/cm}^2$). White arrow (left part of the photo) shows the narrow stripe of damage maximum at the Bragg peak. Right part of the photo predicts with the magnification ($\times 4$) a region marked by rectangle on the left part of the photo.

394 MeV and the ion fluence was $(\Phi \times t)_{\text{Kr}} = 5 \times 10^{12} \text{ ion/cm}^2$. The ion flux was $\Phi_{\text{Kr}} \leq 5 \times 10^9 \text{ ion/cm}^2 \times c$ and the temperature of GaAs samples during irradiation was less than 30°C . The irradiated GaAs samples were cleaved perpendicularly to the irradiated surface (along the projected range of ^{84}Kr ions). The damage depth distribution was visualized by the treatment of cleaves in a special selective chemical solution.

The surface of GaAs sample etched cleaves were studied using a scanning electronic microscope JSM-840 (SEM). The SEM studies showed the absence of radiation damage before the Bragg peak. The structures looked like “channels” were registered far under the Bragg peak (Figs. 1 and 2). The length of zone with visualized “channels” was about a half of ^{84}Kr ion projected ranges. The surface density of “channels” was much less than the track density along the cross section of irradiated crystal should be. This density should be about $N_{\text{cleaves}} \approx \sqrt{(\Phi \times t)_{\text{Kr}}} = 2.236 \times 10^6 \text{ cm}^{-1}$, and the mean distance between the “channels”-tracks should be $R_{\text{track}} \approx 44.7 \text{ \AA}$. It is clear that the observation of such low scale features is impossible using the estimation described above.

In accordance with the SEM results, the radiation damages like “channels” were observed under the Bragg peak and were absent before the Bragg peak where the inelastic energy loss should be high. One can conclude that it is impossible to explain the observed results as occurring owing to ionization losses of ^{84}Kr only. The narrow damage zones with high defect concentration looked like a strongly etched single stripe (Fig. 1) and two stripes (Fig. 2) were observed at the depth of the maximum of nuclear (elastic) energy loss at $Z_{\text{max}} \cong 30.5 \mu\text{m}$. As one can see, the wide etched layer lies under the Bragg peak and is characterized by a width of about $15 \mu\text{m}$ (Fig. 2). So, the damaged zone from the surface up to the end of the etched “channels” spreads up to the depth $Z_{\text{damage}} \cong 1.5 \times R_p = 45 \mu\text{m}$. It is necessary to note that both Figs. 1 and 2 were obtained using different selective chemical etching solutions.

It is necessary to note that the GaAs samples were not oriented in the direction of initial ion beam, i.e. the direct axial ion channeling was excluded.

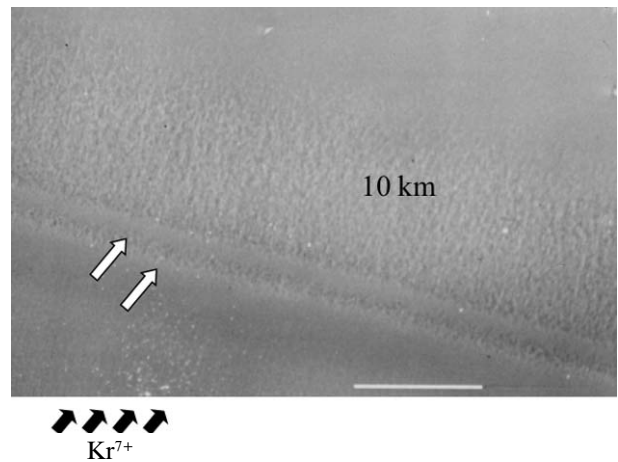


Fig. 2. SEM image of two wide stripes (marked by the white arrows) near the Bragg peak and a wide damage layer with the width of about $15 \mu\text{m}$ under the Bragg peak.

Model of observed damage and discussion

The results of calculations of the value of inelastic energy loss $(-\partial E/\partial Z)_{\text{inel}}^{\text{Kr}} (Z \approx 0)$ and values of damage dose near the surface ($D_{\text{Kr}}(Z \approx 0) = \sigma_d^{\text{Kr}}(Z \approx 0) \times (\Phi \times t)_{\text{Kr}}$) and at the Bragg peak ($D_{\text{Kr}}(Z \approx Z_{\text{max}}) = \sigma_d^{\text{Kr}}(Z \approx Z_{\text{max}}) \times (\Phi \times t)_{\text{Kr}}$) are presented in Table 1. Calculations were carried out using the computer code TRIM-2000 [4].

The maximum energies delivered by ^{84}Kr to firstly knocked Ga and As atoms (FKA) have been calculated using the simple formula:

$$(1) \quad E_{\text{Ga/As}}^{\text{max}} = \frac{4 \times M_{\text{Kr}} \times M_{\text{Ga/As}}}{(M_{\text{Kr}} + M_{\text{Ga/As}})^2} \times E_{\text{Kr}}$$

The projected ranges of FKA in a GaAs target have been calculated using the computer code TRIM-2000 [4]. The maximum energies and projected ranges of FKA are presented in Table 2.

As one can see, the experimentally measured depth position of narrow stripes (Figs. 1 and 2) $Z = 30.5 \mu\text{m}$ is in agreement with the calculated projected range of

Table 1. Energy, fluence, inelastic energy loss, damage doses near the surface ($Z \approx 0 \mu\text{m}$) and in the Bragg peak ($Z \approx Z_{\text{max}}$) of ^{84}Kr ions in a GaAs single crystal

Ion	Energy (MeV)	$(\Phi \times t)_{\text{Kr}}$ (ion/cm ²)	$-(\partial E/\partial Z)_{\text{inel}}^{\text{Kr}}$ ($Z \approx 0$) (keV/nm)	D_{Kr} ($Z \approx 0$) (dpa)	D_{Kr} ($Z \approx Z_{\text{max}}$) (dpa)
^{84}Kr	394	5×10^{12}	15.4	1.75×10^{-4}	1.95×10^{-2}

Table 2. Initial energy of ^{84}Kr ions and maximum transferred energies of knocked out Ga and As ions in the lattice of a GaAs single crystal

Kind of ion	$E_{\text{ion}}^{\text{max}}$ (MeV)	R_p (μm)
^{84}Kr	394.0	30.4×0.7
Ga	389.6	33.7×0.7
As	392.7	32.3×0.6

initial ^{84}Kr ions $R_p^{\text{Kr}} = 30.4 \pm 0.7 \mu\text{m}$. It is clear that the projected ranges of Ga and As FKA with maximum energies are much lower than the maximum depth of the broad damaged zone ($Z_{\text{damage}} \approx 1.5 \times R_p = 45 \mu\text{m}$). So, it is impossible to explain this broad damage layer by the interaction of target with the initial ^{84}Kr ions and firstly knocked Ga and As atoms. For the explanation of the observed experimental results (Figs. 1 and 2) it has been made an assumption that the initial $^{84}\text{Kr}^{7+}$ ions after a few of collisions with GaAs target atoms, as well as firstly knocked Ga and As atoms can be captured by axial or flatness channeling (see, for example, Refs. [8, 12]). Let us discuss such phenomenon in more detail.

As it is well known, the critical angles of axial channeling can be calculated using the expression [8, 12]:

$$(2) \quad \Psi_{\text{crit}} = \begin{cases} \left[\frac{2 \times Z_1 \times Z_2 \times e_0^2}{E_{\text{ion}} \times d} \right]^{1/2} & \text{at } E_{\text{ion}} > \frac{2 \times Z_1 \times Z_2 \times e_0^2 \times d}{a_{\text{T-F}}^2} \\ \left[\frac{1.5 \times Z_1 \times Z_2 \times e_0^2}{E_{\text{ion}} \times d} \times \left(\frac{a_{\text{T-F}}}{d} \right)^2 \right]^{1/4} & \text{at } E_{\text{ion}} < \frac{2 \times Z_1 \times Z_2 \times e_0^2 \times d}{a_{\text{T-F}}^2} \end{cases}$$

Here $d \approx 0.5 \times a_0$ is the distance between atoms along the axis of channeling; a_0 is the lattice constant of crystal; e_0 is the elementary charge of electron; Z_1 and Z_2 are charges of channeling ions and lattice atoms, correspondingly. The parameter $a_{\text{T-F}}$ is the Thomas-Fermi screening radius, i.e. a minimum distance of approach of channeling ions and lattice atoms, which can be represented using the expression [8, 12]:

$$(3) \quad a_{\text{T-F}} = \frac{0.468}{\left[Z_1^{1/2} + Z_2^{1/2} \right]^{2/3}} \text{ \AA}$$

In our case the lattice constant for GaAs crystal with the plane centered cubic lattice and direction [100] is equal to $a_0 = 5.69 \text{ \AA}$. Let us use as estimates of channeling angles the approximation like the mean field ($M-F$). So, one can write:

- 1) for ^{84}Kr ions:
 $Z_1 \equiv Z_{\text{Kr}} = 36$; $Z_2^{M-F} \approx (Z_{\text{Ga}} + Z_{\text{As}})/2 = 32$;

$$a_{\text{T-F}}^{\text{Kr}} \approx 0.09 \text{ \AA}; \quad E_{\text{ion}} = E_{\text{Kr}}^{\text{max}} = 394 \text{ MeV};$$

- 2) for FKA Ga:

$$Z_1 \equiv Z_{\text{Ga}} = 31; \quad Z_2^{M-F} \approx 32; \quad a_{\text{T-F}}^{\text{Ga}} \approx 0.09 \text{ \AA};$$

$$E_{\text{ion}} = E_{\text{Ga}}^{\text{max}} = 389.6 \text{ MeV};$$

- 3) for FKA As:

$$Z_1 \equiv Z_{\text{As}} = 33; \quad Z_2^{M-F} \approx 32; \quad a_{\text{T-F}}^{\text{As}} \approx 0.09 \text{ \AA};$$

$$E_{\text{ion}} = E_{\text{As}}^{\text{max}} = 392.7 \text{ MeV}.$$

For high energy ^{84}Kr ions, the threshold energy value can be calculated using Eq. (2) as:

$$(4) \quad E_{\text{Kr}}^{\text{threshold}} > \frac{2 \times Z_{\text{Kr}} \times Z_2 \times e_0^2 \times d}{a_{\text{T-F}}^2} = 11.7 \text{ MeV}$$

The threshold energy values $E_{\text{Ga}}^{\text{threshold}}$ and $E_{\text{As}}^{\text{threshold}}$ for Ga and As FKA are practically the same. The corresponding minimum critical angles for ^{84}Kr ions and for Ga and As FKA with maximum energies (Table 2) have the values:

$$(5) \quad \Psi_{\text{crit}}^{\text{Kr}}(E_{\text{Kr}}^{\text{max}}) = 0.31^\circ, \quad \Psi_{\text{crit}}^{\text{As}}(E_{\text{As}}^{\text{max}}) = 0.30^\circ, \\ \Psi_{\text{crit}}^{\text{Ga}}(E_{\text{Ga}}^{\text{max}}) = 0.29^\circ$$

It should be noted that the critical angles for capturing of ^{84}Kr ions, Ga and As FKA by axial channeling are significant.

Our estimations allow us to conclude that ^{84}Kr ions after a few collisions with not very high energy delivering in each collision and Ga and As FKA with energies comparable with maximum delivering energies (Table 2) can be captured by the regime of axial channeling if their energies will satisfy the double inequality:

$$(6) \quad E_{\text{Kr}}^{\text{threshold}} < E_M < E_M^{\text{max}}$$

where index $M = \text{Kr, Ga, As}$.

Some authors [9, 10, 16] reported experimental evidence for the redistribution of an isotropic ion flux after transmission through thin crystals. As this observation is established, depending on experimental conditions, there can be strong enhancements, corresponding to the ‘‘transverse cooling’’ or strong reductions, ‘‘transverse heating’’, of the ion flux along a crystal axis or plan (see, as an example, Fig. 3 [9, 10]). One can conclude that after passing of isotropic ion beams through the crystals, a significant number of ions were captured by axis channeling. In Table 3, the kind of ions, their exit energies E_{exit} , kind of crystals and crystal thicknesses are presented together with the final effects (cooling or heating). Here, the terms ‘‘cooling’’ and ‘‘heating’’ effects mean the decreasing of lattice temperature when inelastic energy loss of ions decreases (see Fig. 3, top image) and increasing of lattice temperature in the case of increasing of inelastic energy loss (see Fig. 3, bottom image), correspondingly.

One can conclude that inelastic energy loss of exit Y ions with energies 177, 117 and 63 MeV after passing through a 3.4 μm -thin Si(001) crystal should have the

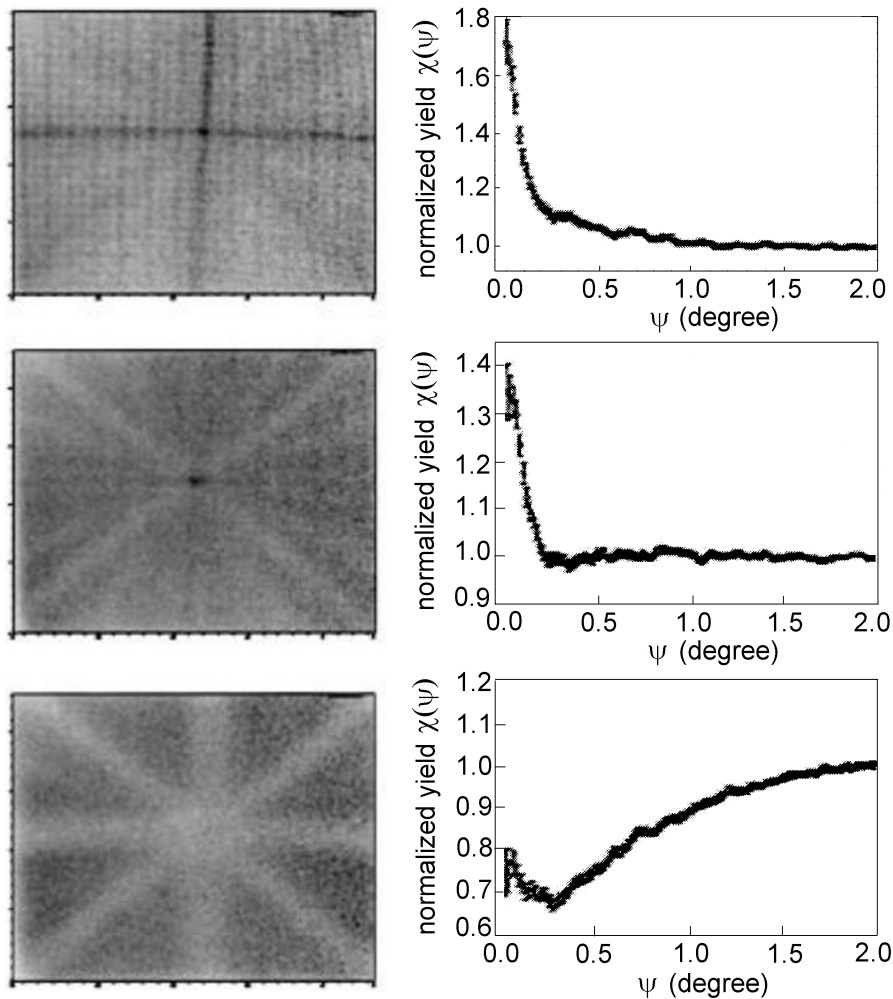


Fig. 3. Angular flux distribution of Y ions after transmission through a 3.4 μm -thin Si(001) crystal, and circular averages around the $\langle 100 \rangle$ axis at varying polar angle. The exit energies are from the top to the bottom, 177, 117, and 63 MeV. The top part shows a clear cooling case, the bottom one is a clear heating case, and the middle part is an intermediate stage. The HWHM of the first two angular distributions are $(0.09 \pm 0.01)^\circ$ and $(0.1 \pm 0.01)^\circ$, the corresponding critical Lindhard angles are 0.23° and 0.28° [9].

Table 3. Kind of ions, their energies, type of crystals in studies [10, 11] with their thicknesses and the kind of interaction of passing ions with all crystals

Number of specimen	Kind of ions	Energy (MeV)	Crystal (axis)	Thickness (μm)	Kind of passing
1	Y (Fig. 3)	177	Si(001)	3.4	Clear cooling case
2	Y (Fig. 3)	117	Si(001)	3.4	Intermediate stage
3	Y (Fig. 3)	63	Si(001)	3.4	Clear heating case
4	Ni	5	Si(110)	2.9	Clearly cooling
5	S	7	Si(110)	–	Overall cooling
6	Ag	66	Ni(001)	1.0	Clear heating case

ratios: 1:1.51:2.81, i.e. the mental projected ranges of ions should have the ratios: 1:0.66:0.36 (see Fig. 3 and Table 3 (1–3 lines)).

Selective chemical etching of GaAs crystal cleaved along projected range of ions

The results of atomic force microscopy (AFM) and selective chemical etching (SCE) for the samples of GaAs irradiated by swift ^{209}Bi heavy ions with energy 710 MeV up to the fluence of 5×10^{10} Bi/cm² were published in [18]. The images of GaAs irradiated surface and the profile of surface realized along the line 1–2 obtained by AFM are presented in Fig. 4.

One can see that the entrances of ^{209}Bi heavy ions to the surface of GaAs samples have circular hillock

forms with a diameter of $D_{\text{hillock}} \approx 15$ nm, height $H_{\text{hillock}} \approx 0.5$ nm with the crater-like structures at the center of each hillock (Fig. 4).

The calculations of temperature inside the ^{209}Bi swift heavy ion track volumes using a thermal spike model and taking into account the dependence of thermophysical parameters vs. temperature and without any free parameters [3, 20] allowed to conclude that the amorphous track volumes can be produced with a maximum radius of about $R_{\text{melt}} \approx 8.8$ nm, this means that the maximum radiuses of melted zones are about 8.8 nm and their existing time is $\tau \approx 8$ ps. Surface density of such hillocks is about 3.5×10^{10} hillock/cm² and this value is in quite good agreement with the ion fluence. SCE allows to observe the steeps of tracks on the splits of GaAs samples irradiated with U (1300 MeV) and Bi (710 MeV) heavy ions at a fluence of 5×10^{10} ions/cm². The track ion

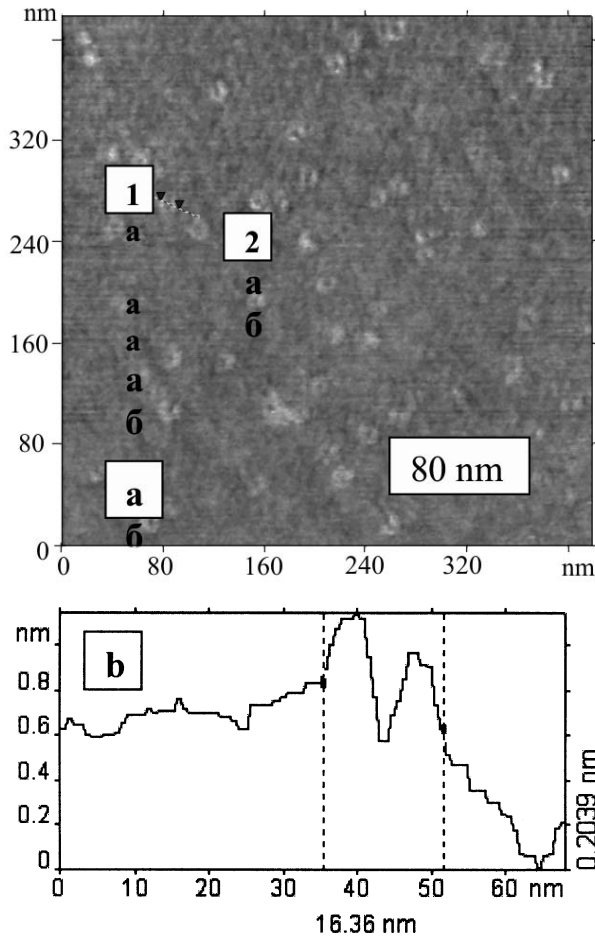


Fig. 4. AFM – lateral-force image of GaAs surface irradiated with ^{209}Bi ions of energy 710 MeV up to the fluence of 5×10^{10} Bi/cm^2 (a) and the profile of surface realized along the line 1–2 (b). The AFM scanning square is equal to $420 \times 420 \text{ nm}^2$.

annealing effect was observed at fluences higher than 1×10^{12} ions/ cm^2 and it was connected with the action of high electronic excitations. One can conclude that the volumes with destroyed (or amorphous) structure are formed along the first ion trajectories where electronic excitations are quite enough for producing hot ion tracks with the inside temperatures (T_{track}) comparable or higher than the melting temperature ($T_{\text{track}} \geq T_{\text{melt}}^{\text{GaAs}} = 1510 \text{ K}$). The high energy δ -electrons should be created with increasing ion fluence near the previously produced ion tracks. The recrystallization processes of such amorphous zones should occur under the influence of δ -electrons if the amorphous phase is not stable. The recrystallization of tracks produced by fullerenes with 30 and 40 MeV energies under the action of electron beam of high voltage microscope was noted in Ref. [20] (transmission electron microscopy method –

TEM). The same effect was registered during the study of Xe track in GaAs (100) by the scanning tunneling method (STM) [11].

The use of SCE allowed us to observe U and Bi ion tracks in GaAs. Nevertheless, the amorphous tracks were not registered by our TEM studies. This may be caused by annealing processes under the influence of electron beam of high voltage electron microscope.

The authors of an excellent paper [11] have investigated the track structures in p-type GaAs bulk crystals irradiated under normal incidence to the (100) $3.54 \text{ GeV Xe}^{31+}$ ions up to the fluence $2.5 \times 10^{11} \div 5.0 \times 10^{11}$ ions/ cm^2 using STM and scanning tunneling spectroscopy (STS) methods. STM images of the cleavage (110) surfaces revealed the fine structure of a single ion track consisting of a long straight linear defect of $D_{\text{core}} \approx 5 \text{ nm}$ in diameter sheathed with a thin fringe in bright contrast. STS study allowed concluding the phase composition, position of Fermi level and local electron density conditions of core and periphery of track. The tracks consist of an amorphous core with a diameter of $D_{\text{core}} \approx 5 \text{ nm}$ surrounded by an irregular region extending over a distance of $\approx 40 \text{ nm}$. The band gap of irregular region surrounding the track core kept the same value as in undamaged matrix, meaning that the crystal structure was preserved into this volume. However, this region is characterized by a different position of the Fermi level relatively to the zone edge and a different local density of state at energetic zones in comparison with undamaged matrix. As it was shown earlier, the AB-etchant ($\text{CrO}_3:\text{H}_2\text{O}:\text{HF}:\text{AgNO}_3$ [6]) is able to reveal areas with changed energetic positions of the Fermi level and local densities of electronic states. We can suppose that selective etching of irradiated samples allows to reveal destroyed areas around the cores of ion tracks.

The energies (E), projected ranges (R_p), inelastic energy loss ($S_{\text{inel}} \equiv -(\partial E/\partial Z)_{\text{inel}}$), damage cross section creation σ_d ($Z \approx 0$) and σ_d ($Z \approx R_p$) for ^{209}Bi , ^{238}U , ^{129}Xe and ^{84}Kr ions at GaAs single crystal are presented in Table 4.

For estimations of maximum lattice temperatures at track axis near the surfaces of GaAs crystal samples for $^{84}\text{Kr}^{36+}$ (394 MeV), $^{129}\text{Xe}^{54+}$ (3.54 GeV) and $^{238}\text{U}^{92}$ (1.3 GeV) was used the simple expression:

$$(7) \quad T_{\text{lattice}}^{\text{ion}} \approx \frac{T_{\text{lattice}}^{\text{Bi}} \times S_{\text{inel}}^{\text{ion}}}{S_{\text{inel}}^{\text{Bi}}}$$

For comparison of temperature effects at ion tracks, it is not so bad approximation, because the temperature dependences and values of thermophysical parameters for electron subsystems are very difficult to be calculated or estimated, so the mistakes in the calculations

Table 4. Kind of used ions in studies, their energies, inelastic energies losses, damage cross sections near the surface ($Z \approx 0 \mu\text{m}$) and in the Bragg peak ($Z \approx Z_{\text{max}}$) all ions and maximum temperatures near the track axis

Kind of ion	Energy (MeV)	R_p (μm)	$S_{\text{inel}}^{\text{ion}}$ (keV/nm)	σ_d ($Z \approx 0$) (dpa \times cm^2/ion)	σ_d ($Z \approx R_p$) (dpa \times cm^2/ion)	T_{lattice} (K)
^{209}Bi	710	34.8	38.3	4.84×10^{-16}	8.83×10^{-15}	2480 [20]
^{238}U	1300	41.2	44.0	2.08×10^{-16}	9.86×10^{-15}	≈ 2850
^{84}Kr	394	30.4	15.4	3.51×10^{-17}	3.87×10^{-15}	≈ 1000
^{129}Xe	3540	178.6	16.1	1.82×10^{-16}	4.17×10^{-15}	≈ 1040

of track temperatures using thermal peak model can be large. The presence of “entrance” places of $^{129}\text{Xe}^{54+}$ swift heavy ions on the surface and long straight linear defects consisting of a core and an irregular region around it, along the projected ranges (cross-sectional method for the study by STM of cleavage surfaces) in spite of the estimations of temperatures on the track axis (see Table 4) allows to conclude that the temperature at ion tracks under the $^{129}\text{Xe}^{54+}$ and $^{84}\text{Kr}^{36+}$ irradiation of GaAs single crystal should be higher than $T_{\text{melt}}^{\text{GaAs}} = 1510$ K.

Conclusion

1. The experimentally measured value of projected range (or more precisely – the position of Bragg peak) of $^{84}\text{Kr}^{7+}$ ions with energy $E_{\text{Kr}} = 394$ MeV in a GaAs single crystal [100] is in agreement with the calculated one.
2. The strong etched zone consisting of two narrow stripes (see Fig. 2) are situated at the distance $\Delta Z \approx 3.1$ μm . The area between the stripes is practically not etched. It can be connected with the so-called thermal spike effects in low-energy single-ion impacts [17, 19].
3. The broad zone of strongly etched structures looked like “channels” lying under the Bragg peak (Figs. 1 and 2) was registered. This may be explained by capturing by regime of axial channeling of ^{84}Kr ions after a few collisions with not very high energy delivering in each collision and Ga and As FKA with high energies ([9, 10, 16], where reported was experimental evidence for the redistribution of an isotropic ion flux after transmission through thin crystals).
4. The absence of etched structures before the Bragg peak may be explained by annealing of previously created ion tracks by following the passage of next ^{84}Kr ions due to thermal spike effect, which can cause heating of lattice up to temperatures sometimes more than the melting temperature of GaAs ($T_{\text{melt}}^{\text{GaAs}} = 1510$ K) [20]).

Acknowledgment. This study was supported in part by the Belarusian Republican Foundation for Fundamental Research (Grant no. T06R-198).

References

1. Alferov ZhI (2002) Double heterostructures: approach and applications in physics, electronics and technologies. *Uspekhi Fizicheskikh Nauk* 172;9:1068–1086 (in Russian)
2. Amirhanov IV, Didyk AYu, Hofman A *et al.* (2006) Sputtering of solids by heavy ions and temperature effects in electronic and lattice subsystems. *Physics Particles and Nuclei* 37;6:837–866
3. Amirhanov IV, Didyk AYu, Muzafarov DZ *et al.* (2008) Application of the thermal spike model for explanation of variations of surface of highly oriented pyrolytic graphite under bombardment by ^{86}Kr and ^{209}Bi ions with high ionization energy loss. *Journal of Surface Investigation. X-ray, Synchrotron and Neutron Techniques* 2;3:331–339
4. Biersack JP, Haggmark LG (1980) A Monte Carlo computer program for the transport of energetic ions in amorphous targets. *Nucl Instrum Meth* 174:257–269
5. Bouneau S, Brunelle A, Della-Negra S *et al.* (2002) Very large gold and silver sputtering yields induced by keV to MeV energy Au_n clusters ($n = 1–13$). *Phys Rev B* 65:114106-1-144106-8
6. Bouneau S, Della-Negra S, Jacquet D *et al.* (2005) Measurements of energy and angular distributions of secondary ions in the sputtering of gold by swift Au_n clusters: study of emission mechanism. *Phys Rev B* 71:174110-1-174106-14
7. Colder A, Marty O, Canut B *et al.* (2002) Latent track formation in germanium irradiated with 20, 30, and 40 MeV fullerenes in electronic regime. *Nucl Instrum Methods Phys Res B* 174:491–498
8. Gemmell DS (1974) Channeling and related effects in the motion of charged particles through crystals. *Rev Mod Phys* 46;1:129–219
9. Gruner F, Assmann W, Bell F *et al.* (2003) Transverse cooling and heating in ion channeling. *Phys Rev B* 68:174104-1-174104-12
10. Gruner F, Schubert M, Assmann W, Bell F, Karamian S, Andersen JU (2002) Transition from transverse cooling to heating. *Nucl Instrum Methods Phys Res B* 193:165–171
11. Hida A, Iwase A, Mera Y, Kambara T, Maeda K (2003) STM study of ion tracks created in GaAs by GeV Xe ion irradiation. *Nucl Instrum Methods Phys Res B* 209:140–144
12. Kalashnikov NP (1981) Coherent interactions of charged particles with single crystals. *Atomizdat, Moscow*
13. Komarov FF (2003) Defect and track formation in solids irradiated by superhigh-energy ions. *Physics-Uspekhi* 46;12:1253–1282
14. Ledentsov NN, Ustinov VM, Schukin VA, Kopiev PS, Alferov ZhI, Bimberg D (1998) Getter-structures with quantum points: creation, properties, laser. *Review. Physics and Technique of Semiconductors* 32;4:385–410
15. Michuskin VM, Sysoev SE, Godeev YuS (2002) Nanostructure creation by ion bombardment of semiconductors and high temperature superconductors. *Bulletin of the Russian Academy of Sciences: Physics (Izvestiya Rossiiskoi Akademii Nauk. Seriya Fizicheskaya)* 66;4:588–592 (in Russian)
16. Shubert M, Gruner F, Assmann W (2003) Transverse cooling and heating of channeled ions and corresponding charge state distributions. *Nucl Instrum Methods Phys Res B* 209:224–232
17. Sigmund P, Claussen C (1981) Sputtering from elastic-collision spikes in heavy-ion-bombarded metals. *J Appl Phys* 52;2:990–993
18. Vlasukova VL, Didyk AYu, Komarov FF, Stukalov OM (2004) GaAs surface structure irradiated by Bi ions with energy 710 MeV. *Bulletin of the Russian Academy of Sciences: Physics (Izvestiya Rossiiskoi Akademii Nauk. Seriya Fizicheskaya)* 68;3:317–319 (in Russian)
19. Yang Q, Li T, King BV, MacDonalds RJ (1996) Thermal spike effects in low-energy single-ion impacts on graphite. *Phys Rev B* 53;6:3032–3038
20. Yuvchenko V (2003) Phase changes and track creation at silicon, irradiated with super-high energy heavy ions. In: *Materials of the 5th Int Conf “Interaction of Radiations with Solids”, October 6–9, 2003 Minsk, Belarus. Belarusian State University, Minsk, pp 38–40*